

The Mark Coventry Award

Articular Contact Estimation in TKA Using In Vivo Kinematics and Finite Element Analysis

Fabio Catani MD, Bernardo Innocenti PhD,
Claudio Belvedere PhD, Luc Labey PhD,
Andrea Ensini MD, Alberto Leardini PhD

Published online: 23 June 2009

© The Association of Bone and Joint Surgeons® 2009

Abstract In vivo fluoroscopy is a well-known technique to analyze joint kinematics of the replaced knee. With this method, however, the contact areas between femoral and tibial components, fundamental for monitoring wear and validating design concepts, are hard to identify. We developed and tested a novel technique to assess condylar and post-cam contacts in TKA. The technique uses in vivo motion data of the replaced knee from standard fluoroscopy as input for finite element models of the prosthesis components. In these models, tibiofemoral contact patterns at the condyles and post-cam articulations were calculated during various activities. To test for feasibility, the technique was applied to a bicruciate posterior-stabilized prosthesis. Sensitivity of the finite element analysis, validation of the technique, and in vivo tests were performed.

To test for potential in the clinical setting, five patients were preliminarily analyzed during chair rising-sitting, stair climbing, and step up-down. For each task and patient, the condylar contact points and contact line rotation were calculated. The results were repeatable and consistent with corresponding calculations from traditional fluoroscopic analysis. Specifically, natural knee kinematics, which shows rolling back and screw home, seemed replicated in all motor tasks. Post-cam contact was observed on both the anterior and posterior faces. Anterior contact is limited to flexion angle close to extension; posterior contact occurs in deeper flexion but is dependent on the motor task. The data suggest the proposed technique provides reliable information to analyze post-cam contacts.

One or more of the authors (BI, LL) are employees of Smith & Nephew, Inc, Memphis, TN.

Each author certifies that his or her institution has approved the human protocol for this investigation, that all investigations were conducted in conformity with ethical principles of research, and that informed consent for participation in the study was obtained.

This work was performed at Istituto Ortopedico Rizzoli (fluoroscopy data collection and analysis) and at the European Center for Knee Research, Smith & Nephew (finite element-based modeling).

F. Catani, A. Ensini
Department of Orthopedic Surgery, Istituto Ortopedici Rizzoli,
Bologna, Italy

C. Belvedere, A. Leardini
Movement Analysis Laboratory, Istituto Ortopedici Rizzoli,
Bologna, Italy

B. Innocenti (✉), L. Labey
European Center for Knee Research, Smith & Nephew, Leuven,
Belgium
e-mail: bernardo.innocenti@smith-nephew.com

Introduction

It is believed the general goals of TKA are achieved by restoring normal knee kinematics. Various methods have been used to analyze the kinematics of both the intact and replaced knee [3, 24, 33]. These methods have included in vitro cadaveric measurements [18, 26, 37], gait analysis with motion systems [2, 3, 42], roentgen stereophotogrammetric analyses [32, 36], quasidynamic MRI testing [23, 29], and in vivo video fluoroscopy [10, 11, 24, 39]. Studies on cadaveric knees suffer from the difficult estimation and setting of the loading conditions in vivo and from the inability of actuators to reproduce loading and motion conditions accurately [12]. Roentgen stereophotogrammetric analyses often have been performed under nonweightbearing conditions but are quasidynamic [32, 35, 36]. Instrumented gait analysis is an easy method for gathering kinematic and kinetic data of the human knee in vivo for noninvasive analyses of its function in

physiologic and various pathologic conditions [17, 26]. However, owing to motion of the skin markers relative to the underlying bone, critical motion artifact may occur [11, 40].

In vivo videofluoroscopy enables the reconstruction of three-dimensional (3D) position and orientation (pose) of the knee prosthesis components more accurately unhindered by the soft tissues around the joint [40]. Registration algorithms estimate the pose of the components from single-plane projection views on fluoroscopic image series [13, 38, 39]. This method has the advantage of testing under in vivo, weightbearing, fully dynamic conditions, while subjects perform various motor tasks. These have included gait [12], stair [15], and deep knee bends [30]. In addition to standard joint kinematics [41], fluoroscopy-based 3D techniques have largely been used to estimate anteroposterior (AP) and mediolateral (ML) displacement of the contact points [8, 9, 24, 27] at each sampled instant (frame), which is important for clinically related observations and deductions, such as restrictions to the range of motion, risks of wear, constraints for joint stability, etc, as well as for supporting novel concepts of TKA design. Although the various techniques proposed differ for a number of features, measurement accuracy for each moving segment is typically from 0.5 to 1.0 mm for translation in the image plane and from 0.5° to 1.0° for rotation. However, in the frequent case of single-plane fluoroscopy, motion perpendicular to the image plane has at best an accuracy in the range of 3.0 to 6.0 mm [5, 6, 19, 25, 31].

Because of this inaccuracy in determining implant pose and because of the complex shape of the components, the identification of the real contact points using fluoroscopy is particularly critical. Frequently, these contact points are assumed to be the closest points to the tibial baseplate of the femoral prosthetic condyles, independent of the shape and position of the polyethylene insert in between [4, 6]. When there is large conformity between the femoral component and the insert, particularly in full extension in a number of designs, the estimation can be even more sensitive to error. In addition, these estimations are obtained frame by frame, independent of previous or following conditions, and as a contact between two rigid bodies, without taking into account the deformation of these objects, which are also loaded in vivo. This also prevents any pressure distribution analysis, particularly relevant for the polyethylene insert. These are all issues typically addressed by finite element (FE) analysis, but rarely has this been utilized in combination with real in vivo replaced knee kinematics [22].

We report here an innovative technique for determining these contact points between the femoral component and the insert in patients with TKA. The technique utilized real in vivo 3D kinematics obtained from fluoroscopy as input

for FE models of the prosthesis specially designed for the purpose. In addition to the commonly used contacts at the femoral prosthetic condyles, the models analyzed the contact between the femoral cam and the tibial post. This technique was used to analyze five patients during chair rising-sitting, stair climbing, and step up-down. The contact points obtained with the innovative technique were compared with those obtained with the traditional “closest point” technique.

Materials and Methods

Five patients affected by primary osteoarthritis received a rotationally unconstrained fixed-bearing prosthesis (Journey® Bi-Cruciate Stabilized Knee System; Smith & Nephew, Inc, Memphis, TN). These patients were selected among those with well-functioning knees and assessed clinically and by videofluoroscopy at 1-year followup. According to the International Knee Society scoring system [28], these were successful implants, with an average score of 163 (standard deviation, 9.1). The overall investigation was conducted in conformity with local ethical regulations; in particular informed consent for participation in the study was obtained from each patient.

Patients were analyzed by videofluoroscopy (digital remote-controlled diagnostic Alpha90SX16; CAT Medical System, Rome, IT) at 10 frames per second during chair rising-sitting, stair climbing, and step up-down. Attention was paid to position the fluoroscopic 32-cm-wide field of view to enable collection of the largest number of images of the replaced knee during the motor task. Two, three, and one repetitions, respectively, were collected for each of these tasks. For the latter, four cycles of up-down motion were collected within a single repetition. The height of the staircase steps was 21 cm. The chair and single-step heights were set for each patient so that he/she started from about 80° and 65° knee flexion, respectively [7]. By means of further images of a 3D cage and a grid of small tantalum beads, a technique for obtaining 3D positions and orientations of the prosthesis components was utilized as described elsewhere [16]. This technique was based on CAD-model shape matching. Relative flexion between the tibial and femoral components was represented using a standard joint convention [21]. With this traditional technique, the condylar contact is assumed to be at a unique contact point on the medial and lateral sides where the minimum distance between the femoral condyles and the tibial baseplate is observed. This also included calculation of the contact line rotation, defined as the rotation on the tibial baseplate of the projection of the line connecting the medial and lateral condylar contact points with respect to the ML axis of the baseplate. This line can show the

instantaneous internal/external rotation angle for the knee. The AP translation of these contact points on this plane was also calculated during the three activities.

The *in vivo* kinematics obtained from fluoroscopy was used as an input for FE models of the implants to calculate condylar contact points between the femoral and tibial components. Initially, a full FE model (Fig. 1A) of the femoral component and polyethylene insert was developed in Abaqus/Explicit™ (Abaqus, Inc, Providence, RI) from the original CAD models of the implant. The femoral component was considered a rigid surface and represented by triangular surface elements (~11,500 elements), and the tibial insert by eight-node 3D hexahedral elements (~15,500 elements). The tibial insert was considered fixed, and the femoral component moved according to the *in vivo* relative kinematics obtained from fluoroscopy. Young's modulus and Poisson ratio assumed for the femoral component were, respectively, 97.905 GPa and 0.3 [45]. The polyethylene insert was treated as a nonlinear elastoplastic material according to literature data [20, 22]. The contact points were determined by the FE software as the centroid of the pressure distribution between the femoral condyles and the tibial insert [1].

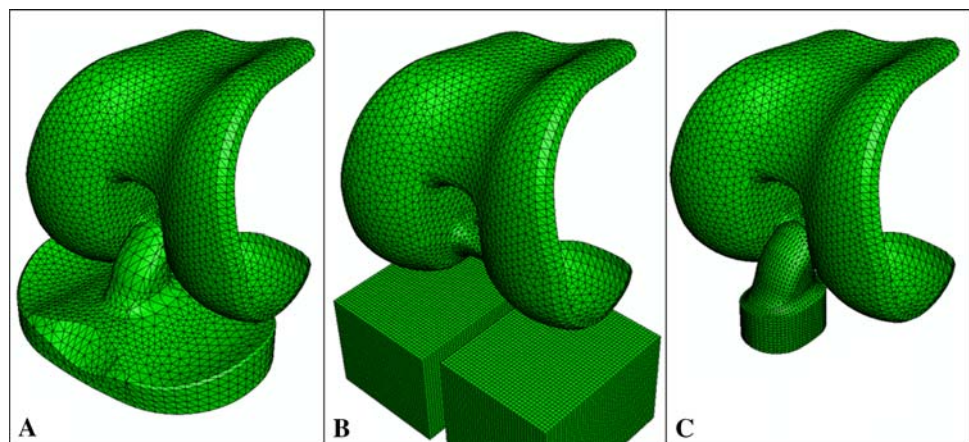
A sensitivity analysis was performed to evaluate the effects of errors in the position of the components intrinsic to the technique of 3D kinematics from the single-plane fluoroscopy. This component position is more critically estimated than any component orientation with this technique. In particular, for each possible "theoretical" original position, ie, the one obtained directly from fluoroscopy-based analysis, four additional positions of the tibial insert were analyzed for 1-mm displacement in the medial, lateral, anterior, and posterior directions. At the four different initial positions, together with the "theoretical" position, the same measured kinematics of the femoral component from fluoroscopy was applied, and the relevant ML and AP displacements of the condylar contact points were compared.

The results of the sensitivity analysis (see Results) showed a different FE model was needed to effectively analyze the contact points (Fig. 1B). The femur model remained the same while each tibial condyle was modeled as a flat box using eight-node 3D hexahedral elements. A similar sensitivity analysis, as described above, demonstrated this model was somewhat insensitive to changes of the model parameters. In particular, a more elastic material produced only larger contact areas but essentially the same location for the centroid of pressure. To avoid large vibration effects on the boxes due to penetration of the femoral condyles, the boxes were assumed to move together with the femoral component in such a way as to maintain a constant penetration of 2 mm.

For each patient and motor task, the medial and lateral contact point coordinates were determined and plotted versus the knee flexion angle. Similar to what is calculated with traditional fluoroscopic-based analysis, the rotation of the contact lines in the tibial baseplate was estimated with their pivot point, ie, the least-square approximation of the intersection of all the contact lines.

This technique was validated using a knee kinematics simulator (Fig. 2). A custom-built six-degrees-of-freedom dynamic knee simulator based on the Oxford rig [14, 34, 44] was used. A loaded squat exercise, until 120° of knee flexion, was simulated. A Journey® Bi-Cruciate Stabilized Knee prosthesis was mounted on the simulator using metal fixtures. Clusters of three markers were attached to the tibial and femoral fixtures to record their movement using four Vicon MX40 motion capture cameras (Vicon, Oxford, UK) with a proven accuracy of 0.3 mm in each direction [43]. The kinematics obtained from the experiment was used as input for the FE model. The contact points coordinates estimated with the FE model were compared with the centroid of pressure obtained using contact pressure sensors (K-Scan® 9000 psi; Tekscan, Inc, South Boston, MA) during the experiment.

Fig. 1A–C Diagrams show the FE models used for the evaluation of the contacts. (A) The full model with the original femoral and tibial components utilized for the sensitivity analysis was then modified to two specialized models: (B) one for the analysis of the condylar contact points and (C) the other for the post-cam contacts.



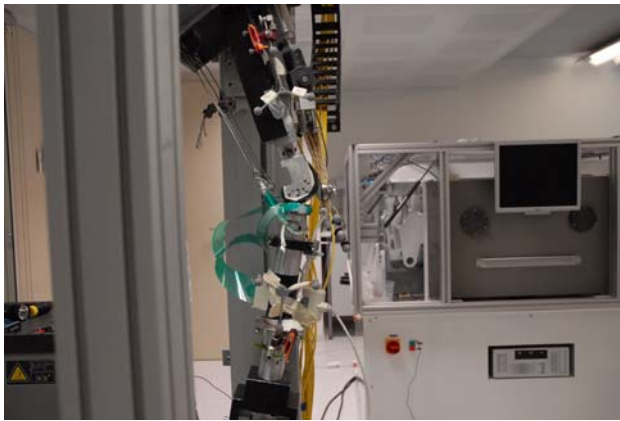


Fig. 2 A photograph shows the experimental setup for the validation of the numerical technique.

A separate FE model was used to analyze post-cam contact. The standard FE model of the femoral component was used together with an original model of the isolated post of the tibial insert (Fig. 1C). The use of only the post instead of the entire tibial insert was chosen to reduce the computational time while maintaining the integrity of the analysis. The fluoroscopy-based kinematics was applied to the femoral component, and the occurrence of contact was evaluated. Three possible situations were considered: anterior contact, posterior contact, and no contact between the cam and the post. Whether there was contact or not was decided based on two criteria. Whenever the contact pressure and/or the contact area at the anterior or posterior

face of the post exceeded a threshold value, 0.05 MPa and 0.25 mm², respectively, the post and cam were considered to be in contact, as determined during a preliminary test.

For this technique, a sensitivity analysis to the AP positioning was also performed. For this purpose, the initial AP position of the post was changed by ± 1 mm and the resulting change in the post-cam contact situation was assessed.

The described FE techniques were used to analyze the original fluoroscopy-based kinematics from the five patients. One representative full cycle of chair rising-sitting, stair climbing, and step up-down at the replaced knee was analyzed. The results were compared with the corresponding measurements from standard fluoroscopy analysis. With this technique, replaced joint kinematics and contacts were consistent among patients.

Results

The analysis of the influence of possible different initial positions (Fig. 3) showed the original full FE model was too sensitive to the inaccuracy in the prosthesis component positions typical of fluoroscopic-based knee kinematics calculation: 1 mm of error in the initial position could induce more than 3 mm of error in the contact point estimation.

The location of the centroid of pressure obtained from the FE model corresponded well with the experimental measurements (Fig. 4), showing a maximum deviation of

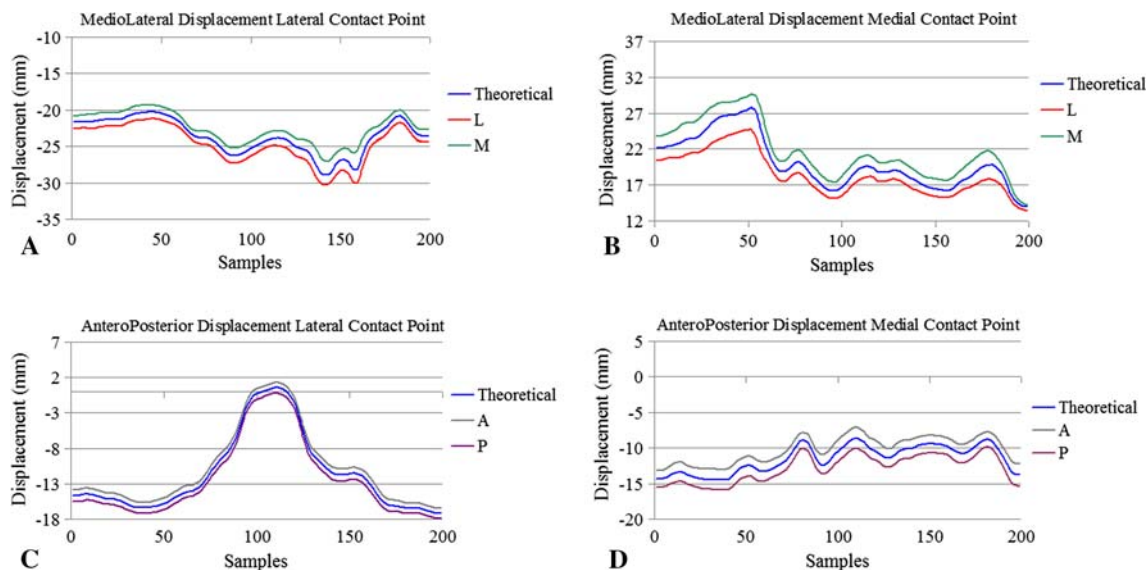


Fig. 3A–D Graphs show the movement of the contact point during the sensitivity analysis: (A) ML movement of the lateral condyle; (B) ML movement of the medial condyle; (C) AP movement of the lateral condyle; and (D) AP movement of the medial condyle. In each graph,

the movement of the contact point for the original “theoretical” location is in blue, the lateral (L) in red, the medial (M) in green, the anterior (A) in grey, and the posterior (P) in purple.

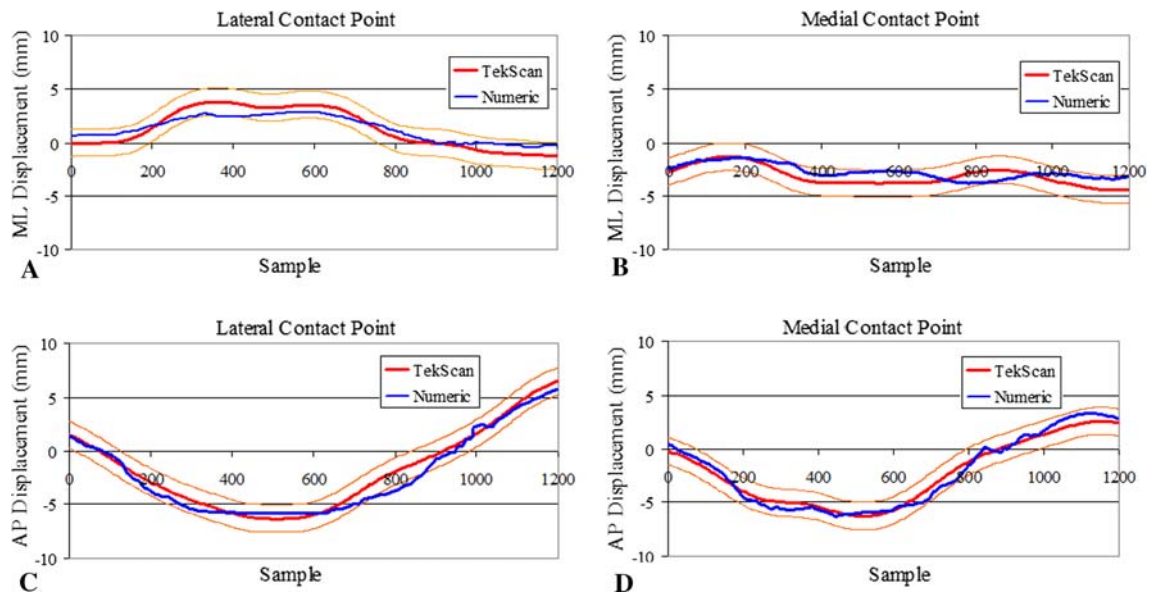
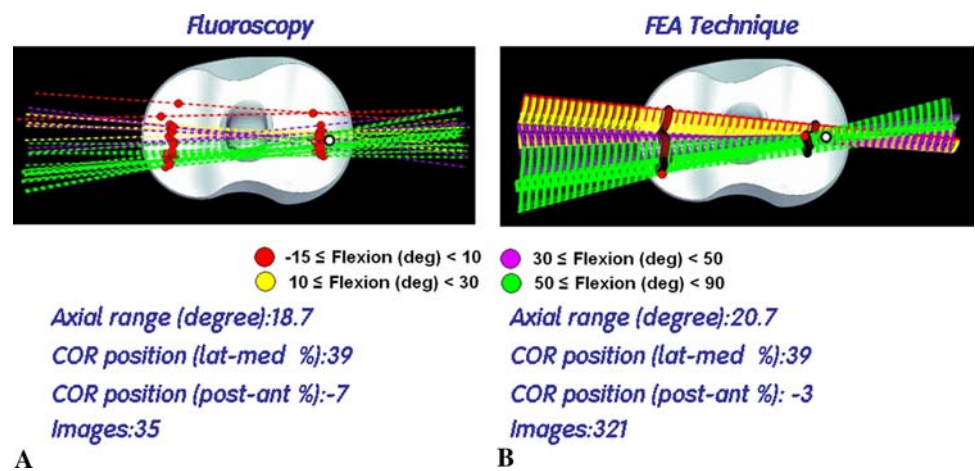


Fig. 4A–D Graphs compare the movements of the centroids of pressure obtained experimentally (Tekscan, in red) and numerically from the FE model (blue). The range of accuracy of the Tekscan sensor is shown in orange. Movements in the (A, B) ML and (C, D) AP directions and of the (A, C) lateral and (B, D) medial condyles are shown.

Fig. 5A–B The contact points location (red dots) and contact line rotation (in different colors according to the corresponding flexion angle) are compared using traditional fluoroscopy (A) and the FE model with fluoroscopy-based kinematics input (B) from a typical patient (Patient A) during chair rising-sitting. For both techniques, the range of the contact line rotation (Axial) and the positions of the pivot point (COR, white dots) are shown.



less than 2 mm. This deviation was within the range of accuracy of the Tekscan sensor (shown in orange; Fig. 4).

FE analysis resulted in a more smooth and continuous motion with respect to the rather discrete and discontinuous pattern from traditional fluoroscopy, resulting in more plausible contact line rotations over time (Fig. 5). Nevertheless, the range of contact line rotation and the location of the pivot point remained nearly the same in the two techniques. This was revealed clearly by the graphs showing the motion of the contact points versus flexion angle (Fig. 6) and the internal/external rotation over time of the contact line (Fig. 7).

Consistent motion patterns were observed for all patients for each motor task (Fig. 8). A larger posterior displacement was observed for the lateral condyle, as a

function of flexion, compared to the medial condyle. This implied replication of the rolling back and screw home mechanisms. Moreover, a ML displacement of both condyles was also seen (Fig. 8). The location of the pivot point was different from patient to patient (Table 1).

FE-based calculations resulted in smooth and consistent patterns of contact also at the post-cam interface; a typical output of this analysis for stair climbing in one patient is shown (Fig. 9). These patterns of post-cam contact in the anterior and posterior areas, in addition to the no-contact condition, along the flexion arc, were found also consistent among patients in all three analyzed motor tasks (Fig. 10). For all three motor tasks, anterior contact was more frequent at small flexion angles (near full extension), and posterior contact occurred in larger flexion. The analysis of

Fig. 6A–D Graphs show the (A, B) ML and (C, D) AP movement of the (A, C) lateral and (B, D) medial contact point versus knee flexion angle as obtained by traditional fluoroscopy (red) and FE (blue) calculations from a typical patient (Patient A) during chair rising-sitting. For comparisons also between sizes, the movements are calculated as percentage of the entire AP length and ML width of the tibial baseplate.

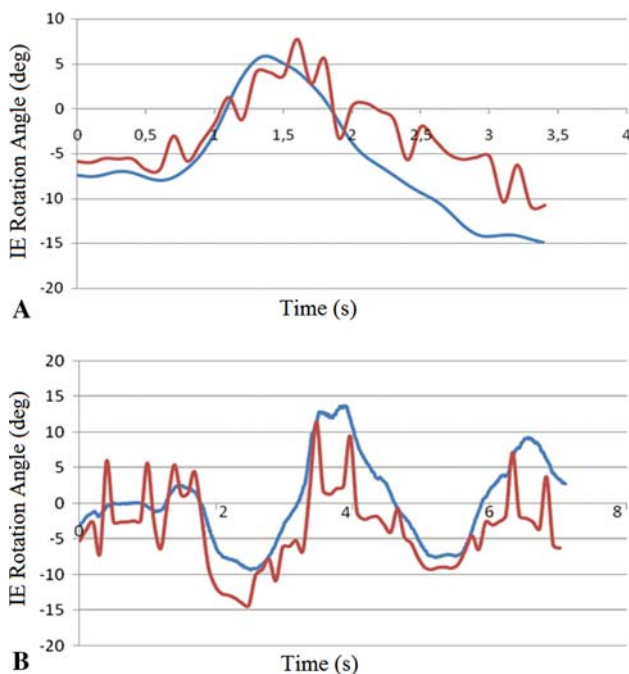
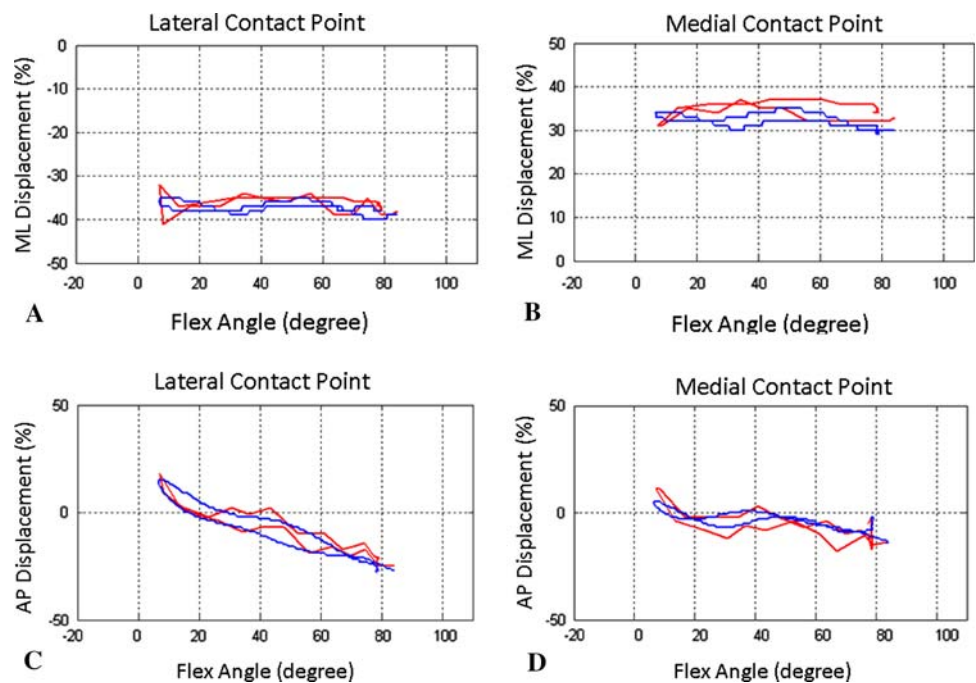


Fig. 7A–B Graphs show rotation over time (in seconds) of the contact line (IE Rotation Angle) as obtained by traditional fluoroscopy (red) and FE (blue) calculations from a typical patient (Patient A) during (A) chair rising and (B) step up-down.

sensitivity to the AP position showed the transition point between two different contact situations in the flexion-extension curve plotted versus time changed by a maximum of 5° . This showed the technique was relatively insensitive to errors of this kind.

Discussion

To overcome the limitations of the traditional 3D fluoroscopic analysis of the joint kinematics in TKA patients and to analyze more reliably contact patterns at these joints, an innovative technique was developed based on FE models. A sensitivity analysis and an experimental validation were performed and reported. In vivo 3D kinematics obtained by fluoroscopy during chair rising-sitting, stair climbing, and step up-down from five patients with a TKA were used as input for these models. The FE technique reproduced well the contact points displacement derived from fluoroscopy but with smoother, more credible and consistent patterns. In addition, for the first time, the models enabled the in vivo analysis of the contact between the femoral cam and the tibial post. Both the condylar and the post-cam contact patterns supported the design features of the analyzed knee implant.

A number of shortcuts were taken in FE modeling to make these calculations feasible and reliable at the same time. The 2-mm constant penetration was taken as a compromise solution between opposite factors after a series of preparatory tests: to avoid separation between the femoral component and insert (which produces no contact estimation during the analysis), a large depth would be required; to reduce vibration effects and the relevant large increase of computational time, a small depth would be recommended. With the penetration used, no relevant differences in the contact point locations were found. Two different criteria were adopted to determine contact between the post and the cam because we wanted to exclude numerical artifacts

Fig. 8A–C Graphs show ML (top row) and AP (bottom) movement of the lateral (left column) and medial (right column) contact points obtained using the FE technique during (A) chair rising-sitting, (B) stair climbing, and (C) step up-down. The means and standard deviations of the five patients are shown versus knee flexion angle taken every 10°.

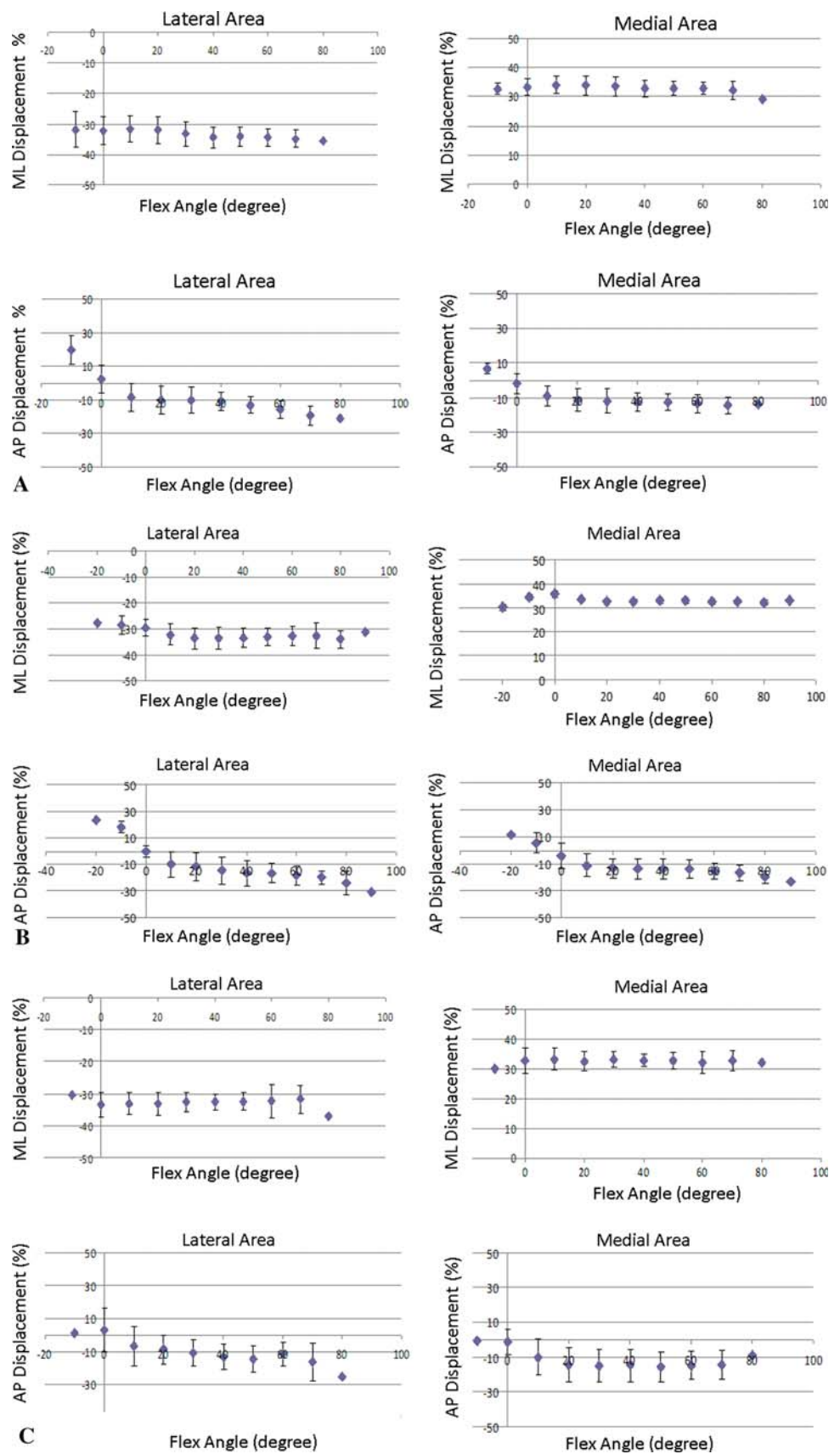
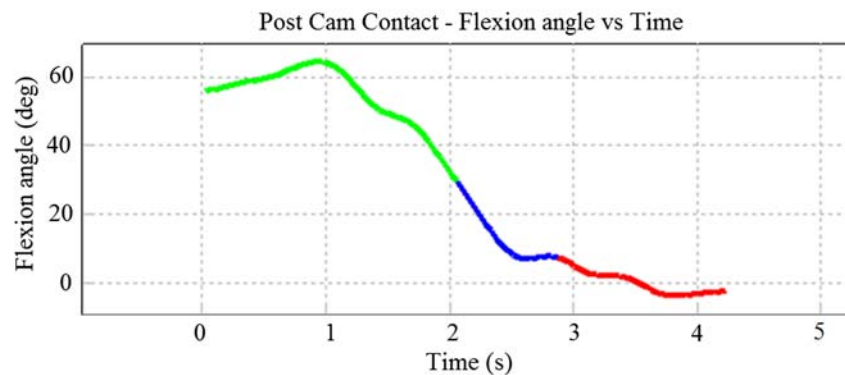


Table 1. Range of rotation of the contact line and location of the pivot point for the five patients and for each motor task

Patient	Amplitude of contact line rotation (°)			Pivot point ML location (%)*			Pivot point AP location (%)*		
	Chair rising-sitting	Stair climbing	Step up-down	Chair rising-sitting	Stair climbing	Step up-down	Chair rising-sitting	Stair climbing	Step up-down
A	20.7	20.5	23	39	59	61	-3	-3	-3
B	15.4	12.5	15.8	98	32	109	-16	-2	-8
C	19.8	4.2	10.5	46	105	68	-19	-19	-19
D	13.4	15.9	6.7	141	69	3	1	3	-13
E	7	20.7	16.6	50	26	54	0	-12	6
Average	15.26	14.76	14.52	74.8	58.2	59	-7.4	-6.6	-9.8

* The location of the pivot point, defined as the least-square approximation of the intersection of all the contact lines, is expressed as a percentage of the overall ML and AP size of the tibial baseplate. The origin is the center of the tibial baseplate; positive directions are laterally and anteriorly. ML = mediolateral; AP = anteroposterior.

Fig. 9 The graph shows the typical output of the post-cam contact analysis with knee flexion angle versus time in stair climbing: posterior contact (green), no contact (blue), and anterior contact (red). Each contact condition and relevant areas are illustrated by the colored drawings of the tibial post.



inherent to FE modeling where a continuous body is discretized in separate elements. This can lead either to virtual contact between single nodes, which is not realistic, or to extremely low pressure values, which are irrelevant. To exclude the former error, we defined a small area threshold; to exclude the latter error, we defined a lower contact pressure threshold. An additional weakness of the study is the limited size of the patient population, although the main aim was to propose and test the technique first; more consistent and robust clinical analyses can now follow. Furthermore, also the acquisition by means of single-plane fluoroscopy could represent a limitation to the study. Nevertheless, past and recent studies have demonstrated the reliability and repeatability of the fluoroscopic technique we utilized [7, 15, 16].

A sensitivity analysis of the technique used was performed. As expected, the intrinsic error of single-plane

fluoroscopy in the prosthesis component positioning, particularly in the ML direction, resulted in a large difference of the condylar contact point locations. Therefore, a number of modifications were made. The complexity of the original shapes of the polyethylene insert was replaced by two independent boxes and a single post. Appropriate mechanical characteristics of the box material were chosen to avoid vibrational effects and distortion of elements and to reduce computational time. An experimental test proved the validity of this approach.

This study is innovative in its combination of in vivo kinematics and FE analysis. The relative motion of the components is the most critical input for the models, considerably affecting the final results. Relative movement data are usually taken from measurements performed with external markers, which are unreliable. On the other hand, fluoroscopy-based kinematics and contact analyses are

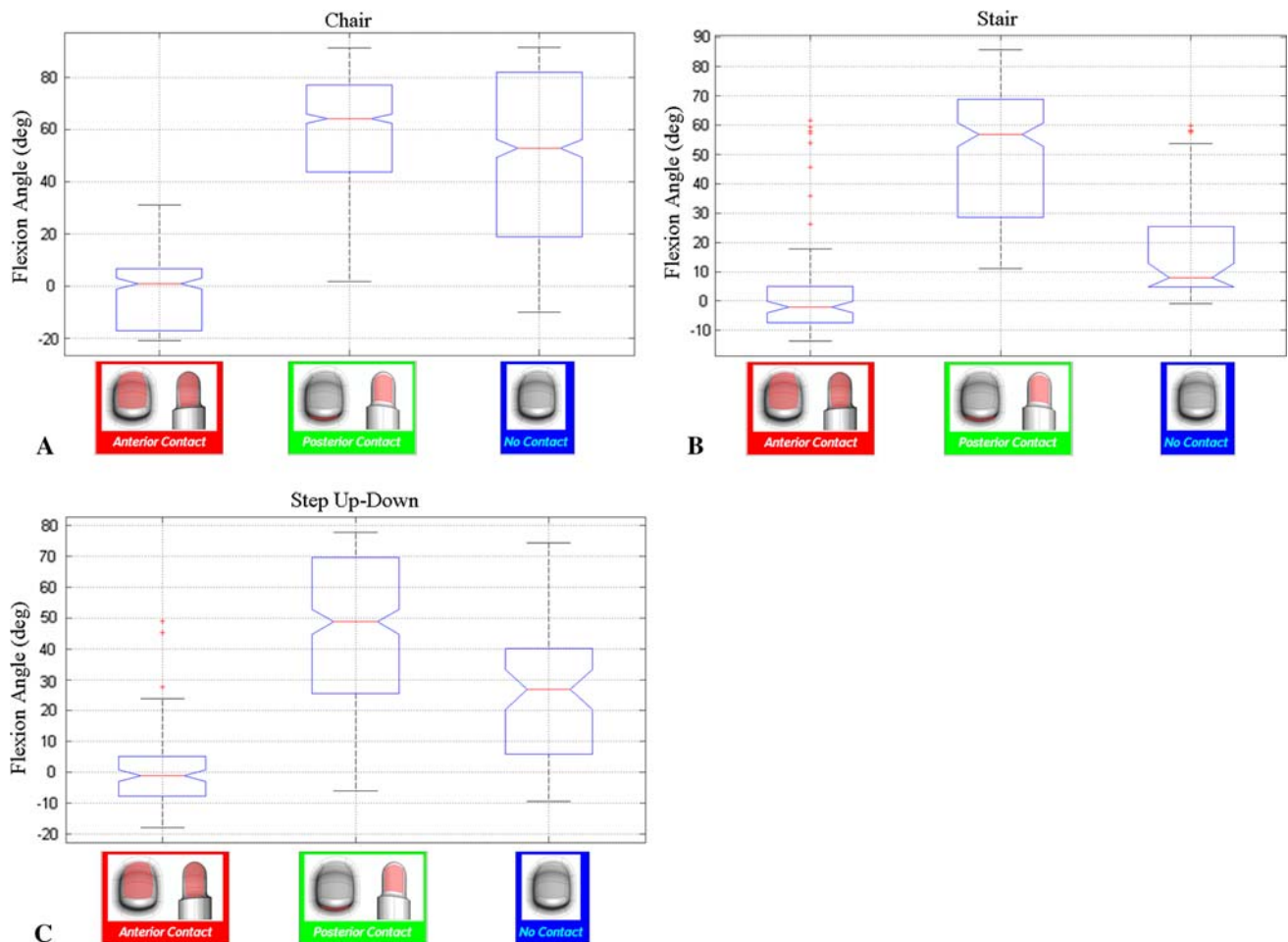


Fig. 10A–C Box and whisker plots for flexion angle distribution for anterior, posterior, and no post-cam contact are shown for (A) chair rising-sitting, (B) stair climbing, and (C) step up-down. Box tops and bottoms are at 25th and 75th percentiles of the samples over the five patients, the distances between these are the interquartile ranges, and

the line in between is the sample median; the variability of the median is depicted by notches. Whiskers are drawn from the ends of the interquartile ranges to the furthest observations within the whisker length. All observations above and below the whiskers are plotted as outliers (red crosses; values >1.5 times the interquartile range).

performed frequently without the support of prosthesis-specific models for the contacts. Our results support the reliability of the traditional measurements based only on fluoroscopy. Nevertheless, the results also demonstrate the necessity of FE models for a more realistic estimation of the condylar contacts and for additional information about in vivo post-cam engagement.

References

1. *ABAQUS Manual: ABAQUS Theory Manual Version 6.5*. Providence, RI: Pawtucket; 2006.
2. Andriacchi TP. Functional analysis of pre- and post knee surgery: total knee arthroplasty and ACL reconstruction. *J Biomech Eng*. 1993;115:575–581.
3. Andriacchi TP, Stanwyck TS, Galante JO. Knee biomechanics and total knee replacement. *J Arthroplasty*. 1986;1:211–219.
4. Banks S, Bellemans J, Nozaki H, Whiteside LA, Harman M, Hodge WA. Knee motions during maximum flexion in fixed and mobile-bearing arthroplasties. *Clin Orthop Relat Res*. 2003;410:131–138.
5. Banks SA. Understanding and interpreting in vivo kinematics studies. In: Bellemans J, Ries MD, Victor J, eds. *Total Knee Arthroplasty: A Guide to Get Better Performance*. Heidelberg, Germany: Springer Verlag; 2005:115–119.
6. Banks SA, Hodge WA. Accurate measurement of three-dimensional knee replacement kinematics using single-plane fluoroscopy. *IEEE Trans Biomed Eng*. 1996;43:638–649.
7. Catani F, Belvedere C, Ensini A, Leardini A, Benedetti MG, Feliciangeli A, Giannini S. In vivo kinematics of guided motion total knee arthroplasty. *Trans Orthop Res Soc*. 2008;33:1987.
8. Chouteau J, Lerat J, Testa R, Moyen B, Banks S. Effects of radiograph projection parameter uncertainty on TKA kinematics from model-image registration. *J Biomech*. 2007;40:3744–3747.
9. Dennis DA, Komistek RD. Kinematics of mobile bearing total knee arthroplasty. In: Bellemans J, Ries MD, Victor J, eds. *Total Knee Arthroplasty: A Guide to Get Better Performance*. Heidelberg, Germany: Springer Verlag; 2005:126–140.

10. Dennis DA, Komistek RD, Colwell CE, Ranawat CS, Scott RD, Thornhill TS, Lapp MA. In vivo anteroposterior femorotibial translation of total knee arthroplasty: a multicenter analysis. *Clin Orthop Relat Res.* 1998;356:47–57.
11. Dennis DA, Komistek RD, Hoff WA, Gabriel SM. In vivo knee kinematics derived using an inverse perspective technique. *Clin Orthop Relat Res.* 1996;331:107–117.
12. Dennis DA, Komistek RD, Mahfouz MR. In vivo fluoroscopic analysis of fixed-bearing total knee replacements. *Clin Orthop Relat Res.* 2003;410:114–130.
13. Dennis DA, Komistek RD, Walker SA, Cheal EJ, Stiehl JB. Femoral condylar lift-off in vivo in total knee arthroplasty. *J Bone Joint Surg Br.* 2001;83:33–39.
14. Ezzet KA, Hershey AL, D'Lima DD, Irby SE, Kaufman KR, Colwell CW Jr. Patellar tracking in total knee arthroplasty: inset versus onset design. *J Arthroplasty.* 2001;16:838–843.
15. Fantozzi S, Benedetti MG, Leardini A, Banks SA, Cappello A, Assirelli D, Catani F. Fluoroscopic and gait analysis of the functional performance in stair ascent of two total knee replacement designs. *Gait Posture.* 2003;17:225–234.
16. Fantozzi S, Catani F, Ensini A, Leardini A, Giannini S. Femoral rollback of cruciate-retaining and posterior-stabilized total knee replacements: in vivo fluoroscopic analysis during activities of daily living. *J Orthop Res.* 2006;24:2222–2229.
17. Feng EL, Stulberg SD, Wixson RL. Progressive subluxation and polyethylene wear in total knee replacements with flat articular surfaces. *Clin Orthop Relat Res.* 1994;299:60–71.
18. Fukubayashi T, Torzilli PA, Sherman MF, Warren RF. An in vitro biomechanical evaluation of anterior-posterior motion of the knee: tibial displacement, rotation, and torque. *J Bone Joint Surg Am.* 1982;64:258–264.
19. Fukuoka Y, Hoshino A, Ishida A. Accurate 3D pose estimation method for polyethylene wear assessment in total knee replacement. *Conf Proc IEEE Eng Med Biol Soc.* 1997;4:1849–1852.
20. Godest AC, Beaugonin M, Haug E, Taylor M, Gregson PJ. Simulation of a knee joint replacement during a gait cycle using explicit finite element analysis. *J Biomech.* 2002;35:267–275.
21. Grood ES, Suntay WJ. A joint coordinate system for the clinical description of three-dimensional motions: application to the knee. *J Biomech Eng.* 1983;105:136–144.
22. Halloran JP, Petrella AJ, Rullkoetter PJ. Explicit finite element modeling of total knee replacement mechanics. *J Biomech.* 2005;38:323–331.
23. Hill PF, Vedi V, Williams A, Iwaki H, Pinskerova V, Freeman MA. Tibiofemoral movement 2: the loaded and unloaded living knee studied by MRI. *J Bone Joint Surg Br.* 2000;82:1196–1200.
24. Hoff WA, Komistek RD, Dennis DA, Gabriel SA, Walker SA. A three dimensional determination of femorotibial contact positions under in vivo conditions using fluoroscopy. *J Clin Biomech.* 1998;13:455–470.
25. Hoff WA, Komistek RD, Dennis DA, Walker S, Northcut E, Spargo K. Pose estimation of artificial knee implants in fluoroscopy images using a template matching technique. In: *Proceedings of the Third IEEE Workshop on Applications of Computer Vision.* New York, NY: IEEE; 1996:181–186.
26. Hsieh HH, Walker PS. Stabilizing mechanisms of the loaded and unloaded knee joint. *J Bone Joint Surg Am.* 1976;58:87–93.
27. Incavo SJ, Mullins ER, Coughlin KM, Banks S, Banks A, Beynon BD. Tibio-femoral kinematic analysis of kneeling after total knee arthroplasty. *J Arthroplasty.* 2004;19:906–910.
28. Insall JN, Dorr LD, Scott RD, Scott WN. Rationale of the Knee Society clinical rating system. *Clin Orthop Relat Res.* 1989;248:13–14.
29. Iwaki H, Pinskerova V, Freeman MA. Tibiofemoral movement 1: the shapes and relative movements of the femur and tibia in unloaded cadaver knee. *J Bone Joint Surg Br.* 2000;82:1189–1195.
30. Kanekasu K, Banks SA, Honjo S, Nakata O, Kato H. Fluoroscopic analysis of knee arthroplasty kinematics during deep flexion kneeling. *J Arthroplasty.* 2004;19:998–1003.
31. Kanisawa I, Banks AZ, Banks SA, Moriya H, Tsuchiya A. Weight-bearing knee kinematics in subjects with two types of anterior cruciate ligament reconstruction. *Knee Surg Sports Traumatol Arthrosc.* 2003;11:16–22.
32. Karrholm J, Brandsson S, Freeman MA. Tibiofemoral movement 4: changes of axial tibial rotation caused by forced rotation at the weight-bearing knee studied by RSA. *J Bone Joint Surg Br.* 2000;82:1201–1203.
33. Lafortune M, Cavanagh P, Sommer HJ 3rd, Kalenak A. A three-dimensional kinematics of the human knee during walking. *J Biomech.* 1992;25:347–357.
34. Mountney J, Wilson DR, Paice M, Masri BA, Greidanus NV. The effect of an augmentation patella prosthesis versus patelloplasty on revision patellar kinematics and quadriceps tendon force: an ex vivo study. *J Arthroplasty.* 2008;23:1219–1231.
35. Nilsson KG, Karrholm J, Ekelund L. Knee motion in total knee arthroplasty: a roentgen stereophotogrammetric analysis of the kinematics of the Tricon-M knee prosthesis. *Clin Orthop Relat Res.* 1990;256:147–161.
36. Nilsson KG, Karrholm J, Gadegaard P. Abnormal kinematics of the artificial knee: roentgen stereophotogrammetric analysis of 10 Miller-Galante and five New Jersey LCS knees. *Acta Orthop Scand.* 1991;62:440–446.
37. Oishi CS, Kaufman KR, Irby SE, Colwell CW Jr. Effects of patellar thickness on compression and shear forces in total knee arthroplasty. *Clin Orthop Relat Res.* 1996;331:283–290.
38. Stiehl JB, Dennis DA, Komistek RD. Detrimental kinematics of a flat on flat total condylar knee arthroplasty. *Clin Orthop Relat Res.* 1999;365:139–148.
39. Stiehl JB, Dennis DA, Komistek RD, Crane H. In vivo determination of condylar liftoff and screw home in a mobile bearing total knee arthroplasty. *J Arthroplasty.* 1999;14:293–299.
40. Stiehl JB, Komistek RD, Dennis DA, Paxson RD, Hoff WA. Fluoroscopic analysis after posterior cruciate retaining knee arthroplasty. *J Bone Joint Surg Br.* 1995;77:884–889.
41. Tupling SJ, Pierrynowski MR. Use of cardan angles to locate rigid bodies in three-dimensional space. *Med Biol Eng Comput.* 1987;25:527–532.
42. Wilson SA, McCann PD, Gotlin RS, Ramakrishnan HK, Wootten ME, Insall JN. Comprehensive gait analysis in posterior-stabilized knee arthroplasty. *J Arthroplasty.* 1996;11:359–367.
43. Windolf M, Götzen N, Morlock M. Systematic accuracy and precision analysis of video motion capturing systems—exemplified on the Vicon-460 system. *J Biomech.* 2008;41:2776–2780.
44. Zavatsky AB. A kinematic-freedom analysis of a flexed-knee-stance testing rig. *J Biomech.* 1997;30:277–280.
45. Zirconium Products: Technical Data Sheet; 2003. Wah Chang: An Allegheny Technologies Company. Available at: http://www.wahchang.com/pages/products/data/pdf/Zr_Products_Zr702_705.pdf 2003. Accessed February 2009.